

---

# Latent Neural Operator for Solving Forward and Inverse PDE Problems

---

**Tian Wang**

Institute of Automation,  
Chinese Academy of Sciences  
University of Chinese Academy of Sciences  
wangtian2022@ia.ac.cn

**Chuang Wang**

Institute of Automation,  
Chinese Academy of Sciences  
University of Chinese Academy of Sciences  
wangchuang@ia.ac.cn

## Abstract

Neural operators effectively solve PDE problems from data without knowing the explicit equations, which learn the map from the input sequences of observed samples to the predicted values. Most existed works build the model in the original geometric space, leading to high computational costs when the number of sample points is large. We present the Latent Neural Operator (LNO) solving PDEs in the latent space. In particular, we first propose Physics-Cross-Attention (PhCA) transforming representation from the geometric space to the latent space, then learn the operator in the latent space, and finally recover the real-world geometric space via the inverse PhCA map. Our model retains flexibility that can decode values in any position not limited to locations defined in training set, and therefore can naturally perform interpolation and extrapolation tasks particularly useful for inverse problems. Moreover, the proposed LNO improves in both prediction accuracy and computational efficiency. Experiments show that LNO reduces the GPU memory by 50%, speeds up training 1.8 times, and reaches state-of-the-art accuracy on four out of six benchmarks for forward problems and a benchmark for inverse problem.

## 1 Introduction

Neural network approaches for partial differential equations (PDEs) attract increasing attentions in diverse scientific fields, for instance, meteorological prediction[1], industrial design[2], geological sensing[3] and environmental monitoring[4] to name a few. Compared with traditional numerical methods, *e.g.*, finite element method[5], which demands large amount of computational resources and requires meticulous discretization involving a lot of specialized knowledge, neural networks provide a new paradigm for solving PDE-driven problems with better trade-off between accuracy and flexibility.

Neural PDE solvers can be divided into two main categories, physics-informed and operator-learning models. The physics-informed methods[6–11] enforce the inductive bias of explicit PDE instances into loss function or model architecture, usually yielding solutions with high accuracy, but are less flexible as they require fresh training to find the solution for each new instance. In contrast, the operator learning methods[12–15] adopt a data-driven paradigm to learn the implicit PDE constraint from pair of samples representing input-to-output functional mappings, providing better flexibility that can generalize to different initial/boundary conditions beyond the scope of the training data, but have yet large room to improve in the prediction accuracy.

Recently, Transformers[16] are prevailing in neural operator structures. Theoretically, attention mechanism was proved to be a special form of the integral kernel[15, 17] in neural operator, which naturally conforms to sequence-to-sequence characterization. Moreover, the fully-connected attention

structure enables the model characterizes long-distance and quadratic relationship among sample points, which yields more accurate prediction than the vanilla MLP structure[13] but at an expense of increasing the computational complexity drastically, as the complexity is quadratic respect to the length of input sequence.

To alleviate the complexity, existing works employed linear attention mechanism [18–21] speeding up the computation but sacrificing precision due to their limited expressive power. Another lines of works attempted to solve the PDE in latent space with small number of samples [22–24], which get rid of abundant sample points in the original geometric space and capture physical correlations in the tighter latent space.

In this work, we present the Latent Neural Operator (LNO) with particular effort on designing the **Physics-Cross-Attention (PhCA)** module to learn the latent space to optimize the trade-off between accuracy and flexibility, and reduce the computational complexity as well. Specifically, LNO first encodes the input sample sequence into a learnable latent space by PhCA. Then, the model learns the PDE operator in the latent space via a stack of Transformer layers. Finally, the predicted output function is decoded by the inverse PhCA, given any query locations. Unlike previous works that either pre-define the latent space as frequency domain [14], or switch back-and-forth between latent space and geometric space at each layer [23], the latent space of the LNO is learnable from data and the data are only transformed at the first and last layer.

The proposed PhCA module decouples the locations of input samples fed in the encoder and output samples fed in the decoder, which can predict values in any position not limited by the observation. Therefore, it can naturally perform interpolation and extrapolation tasks, which is fundamental for solving inverse problems. The proposed LNO improves in both prediction accuracy and computational efficiency. Experiments shows that LNO reduces the GPU memory by 50% and speeds up training 1.8 times. Moreover, it reaches state-of-the-art accuracy on four (Pipe, Elasticity, Darcy, Navier-Stokes) out of six benchmarks for forward problems and a benchmark for inverse problem on Burgers’ equation.

Finally, the main contributions of our LNO framework are summarized as follow.

- **Flexibility:** We propose Physics-Cross-Attention (PhCA) module which decouples the locations of input and output samples and learns the latent space from data. We also build the Latent Neural Operator (LNO) model for solving both forward and inverse PDE problems.
- **Efficiency:** The LNO model transforms the data to the latent space only once. Compared with other approaches that switch the latent space and geometric space in each Transformer layer, the proposed model reduces complexity drastically in term of GPU memory usage, training time and number of model parameters.
- **Accuracy:** We obtain state-of-the-art results on the forward problems of Pipe, Elasticity, Darcy, Navier-Stokes, and the inverse problem of Burgers’ equation.

## 2 Related works

We first review two major classes of neural PDE approaches, physics-informed and operator-learning methods. Then, we briefly discuss the works using neural networks for solving inverse PDE problems.

### 2.1 Physics-Informed Machine Learning

Physics-informed machine learning methods incorporate prior knowledge of PDEs into loss function or model architecture. The Physics-Informed Neural Network (PINN)[7] and its variants are among the most classic methods. PINN integrates the differential equation, initial conditions and boundary conditions into the loss function, guiding the neural network to approximate the solution by ensuring its derivatives satisfies the equation and the output aligns with the initial and boundary conditions. Other methods attempt to encode physical priors into the model architecture, *e.g.*, the Finite Element Neural Network (FINN)[8] and Physics-encoded Recurrent Convolutional Neural Network (PeRCNN)[10]. These methods achieve high precision, but require solving optimization to train the networks for each instance. In addition, in the case, where concrete PDE is unknown or not

exact, it is challenging to adopt those methods, limiting the generalization ability and flexibility in practical data-rich situations.

## 2.2 Operator Learning

Operator learning methods aim to find a functional map from coefficients, forcing terms and initial conditions to the solution function by learning an approximating operator. These methods train neural networks to capture the correspondence between input and output functions from data without needing to know the underlying PDE explicitly. DeepONet[13, 25] first introduces approximating operators using neural networks.

A series of kernel integral operator forms were proposed to model the mappings between functions as neural operators[26, 14, 15]. Specifically, Galerkin Transformer[20] utilizes Galerkin-type attention mechanism as kernel integral operators. OFormer[27] improves Galerkin-type attention by decoupling observation positions and query positions through cross attention. GNOT[21] introduces heterogeneous cross attention to modulate various input conditions for query positions, and alleviates computational pressure of the large grid by linear-time-complexity attention mechanism. FactFormer[28] proposes axial factorized kernel integral, decomposing input functions into multiple one-dimensional sub-functions, effectively reducing computation. ONO[29] enhances the generalization of neural operators by adding orthogonality regularization in attention mechanisms.

Researchers also explored the idea of modeling in latent space. Transolver[23] employs Physics-Attention in each layer to map back-and-forth between geometric features and physical features. LSM[22] encodes the input function into the latent space using cross-attention, constructs orthogonal basis, and then decodes the solution back to the geometric space through cross-attention again. UPT[24] introduces encoding and decoding losses, compresses geometric point information into super-node information in latent space via graph neural network[30].

Compared with existing methods, we autonomously learn mappings between functions in real-world space and the latent space in an end-to-end fashion with the cross-attention mechanism, without manually constructed orthogonal basis nor additionally introduced loss.

## 2.3 Inverse Problem

Inverse problems of PDEs have extensive applications in fields involving sensing and reconstruction such as medical imaging and geological sensing. For instance, Transformer-based deep direct sampling methods[31] have been proposed for electrical impedance tomography, and convolutional network methods[32–34] are widely used in full waveform inversion.

Theoretical works on solving inverse problems have also been proposed. The reconstruction of diffusion fields with localized sources have been studied[35] from the perspective of sampling matrix in spatiotemporal domain. PINN[36–38] approximates the solution based on partially observed data to compute the unknown data. NIO[39] combines DeepONet[13] and FNO[14] to construct a framework for solving inverse problems. FINN[8, 40] sets boundary conditions as learnable parameters, and infer boundary values through backpropagation. We aim to unify the solution of forward and inverse problems in the latent space through the PhCA module, which decouples observation and prediction positions.

# 3 Method

We formally define both the forward and the inverse problems of PDEs. Then, we introduce our Latent Neural Operator (LNO) model. Finally, we discuss the core module that learns transformation between real-world space and latent space via cross-attention mechanism.

## 3.1 Problem Setup

We consider a partial differential equation (PDE) with boundary and/or initial conditions defined on  $D \subseteq \mathbb{R}^d$  or  $\mathbb{R}^d \times [0, T]$

$$\begin{aligned} \mathcal{L}_a \circ u &= 0, \\ u(x) &= b(x), \quad x \in \partial D \end{aligned} \tag{1}$$

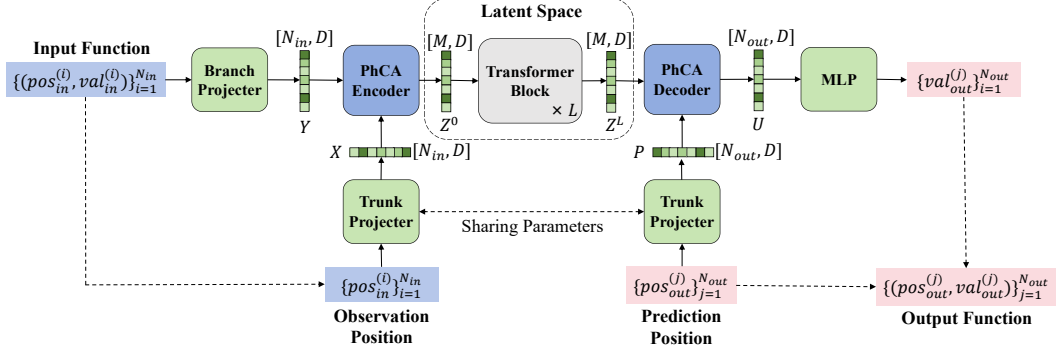


Figure 1: The overall architecture of Latent Neural Operator.

where  $\mathcal{L}_a$  is an operator containing partial differentials parameterized by a set of coefficients  $a$ , and  $u(x)$ ,  $x \in D$  and  $b(x)$  represent the solution to the PDE and the boundary/initial conditions respectively.

A conventional forward problem aims to find the solution  $u(x)$ , given the differential operator  $\mathcal{L}_a$  in (1) with the explicit parameters  $a$  and the boundary/initial conditions  $b(x)$ . For an inverse problem, given an observed set of partial data  $\{(x, u(x)) | x \in \tilde{D} \subset D\}$ , the task is to infer the PDE that generates the observed data along with possible boundary/initial conditions or the parameters  $a$  in the differential operator  $\mathcal{L}_a$ .

Both forward and inverse problems can be unified as an operator learning task fitting into a sequence-to-sequence translation framework. An operator model estimates the mapping  $\mathcal{F} : h \mapsto g$  from an input function  $h$  to an output function  $g$  by the data-driven approach using paired training data of input-output sequences  $(\{h(y_i)\}_i, \{g(z_j)\}_j)$ .

Specifically, for the forward problem, the inputs are samples of either boundary/initial function  $b$  or PDE coefficient function  $a$ , and the output are the physical quantity  $u$  evaluated at a grid of points. Conversely, for the inverse problem, the input are a few partially observation samples  $\{(pos_{in}^{(i)}, val_{in}^{(i)})\}_{i=1}^{N_{in}} = \{(x_i, u(x_i))\}_{i=1}^{N_{in}}$ , and the outputs are boundary/initial function (e.g., infer initial state) or the PDE coefficient function (also coined as system identification problem).

The challenge in solving forward and inverse problems of PDEs lies in the large lengths of input and output sequences. In terms of operator approximating, complex kernel integrals lead to high computational cost while simple kernel integrals lack in accuracy. In this work, we build accurate and computationally efficient model for both forward and inverse problem by learning the operator in the learnable latent space.

### 3.2 Latent Neural Operator

**Overview** The proposed model of Latent Neural Operator (LNO) is applicable for both forward and inverse PDE problems. It consists of four modules: an embedding layer to lift the dimension of the input data, an encoder to transform the input data to a learnable latent space, a sequence of self-attention layers for modeling operator in the latent space, and a decoder to recover the latent representation to the real-world space. The overall architecture of LNO is shown in Figure 1

**Embedding inputs** First, we embed the positions and physics quantities of the input sequence to a higher dimensional representation. It is implemented by two MLPs, where the first only embeds the position information and the second embeds both the location and physics quantities

$$\begin{aligned} x^{(i)} &= \text{trunk-projector}(pos_{in}^{(i)}), & x^{(i)} &\in \mathbb{R}^{d \times 1} \\ y^{(i)} &= \text{branch-projector}(\text{concat}(pos_{in}^{(i)}, val_{in}^{(i)})), & y^{(i)} &\in \mathbb{R}^{d \times 1}. \end{aligned}$$

Analogous to DeepONet [13], we named these MLPs as trunk-projector and branch-projector respectively. The embedding operation helps to map the locations and physics quantities to the space where their relationships are easier to be captured.

**Encoding to latent space** We seek the representation of the input function in a latent space, where the number  $M$  of sample points in the latent space can be much smaller than the number  $N_{in}$  of samples of raw inputs. We use the cross-attention to model space transformation, where the query  $\mathbf{H}$ , key  $\mathbf{X} = [x^{(1)}, x^{(2)}, \dots, x^{(N_{in})}]^T$  and value  $\mathbf{Y} = [y^{(1)}, y^{(2)}, \dots, y^{(N_{in})}]^T$  inputs corresponding to locations in the target latent space, embedding of locations in the source real-world space, and embedding of locations and physics quantities in the source real-world respectively

$$\mathbf{Z}^0 = \text{Physics-Cross-Attention}(\mathbf{H}, \mathbf{X}, \mathbf{Y}) \quad (2)$$

In contrast to FNO[14], where the latent space is pre-defined as the frequency domain, we learn the latent space from data. Therefore, the sample locations  $\mathbf{H}$  as query in the cross-attention are also learnable parameters.

After encoding the input function into the latent space, the length of the sequence to be processed is reduced from  $N_{in}$  to  $M$ . With  $M \ll N_{in}$ , extracting the feature of the input function in the latent space will be much more efficient than in the real-world geometry space.

**Learning operator in the latent space** We model the operator of the forward/inverse PDE problem in the latent space, using a stack of Transformer blocks with self-attention mechanism

$$\mathbf{Z}^l = \text{MLP}(\text{LayerNorm}(\hat{\mathbf{Z}}^l)) + \hat{\mathbf{Z}}^l \quad \text{with } \hat{\mathbf{Z}}^l = \text{Attention}(\text{LayerNorm}(\mathbf{Z}^{l-1})) + \mathbf{Z}^{l-1}$$

where  $l \in \{1, 2, \dots, L\}$  is the index of Transformer block with  $L$  being the number of the blocks. We experiment several implementations of attention mechanisms in the ablation study, and find the classical scaled dot-product attention [16] performs consistently well on various tasks.

**Decoding to real-world space** Finally, we decode the output sequence from the latent sequence through Physics-Cross-Attention according to the query  $pos_{out}$  of the output sample locations, and use another MLP to map the embeddings to the values of output function

$$\begin{aligned} p^{(j)} &= \text{trunk-projector}(pos_{out}^{(j)}), & p^{(j)} &\in \mathbb{R}^{d \times 1} \\ \mathbf{U} &= \text{Physics-Cross-Attention}(\mathbf{P}, \mathbf{H}, \mathbf{Z}^L) & (3) \\ val_{out}^{(j)} &= \text{MLP}(u^{(j)}), & u^{(j)} &\in \mathbb{R}^{d \times 1} \end{aligned}$$

During the inferring phase, the trunk-projector can accept inputs from any position, enabling LNO generalize to unseen region where the positions are not presented in training phase.

### 3.3 Physics Cross Attention

The **Physics-Cross-Attention** (PhCA) is the core module in the aforementioned latent neural operator (LNO) model, acted as the encoder and decoder which transform the data representation back-and-forth between the real-world space and the latent space. Motivated by the work [21] that learns the operator mapping cross domains using the cross-attention, we use the same cross-attention to model the transformation to/from the latent space, but set the latent space learnable rather than pre-defined, *e.g.*, FNO [14].

In particular, the rows of the query  $\mathbf{H}$  and key  $\mathbf{X}$  matrices in (2) represent the embedded positions of samples in the target and source space respectively. A row of the value matrix  $\mathbf{Y}$  is the embedding of both position and physics quantity of a sample in the source space. We design the latent space to be learned from data. Thus, the positions  $\mathbf{H}$  of samples in the latent space should be set as learnable parameters as well. Then, the cross-attention of the encoder in (2) is simplified as

$$\mathbf{Z}^0 = \text{softmax}\left(\frac{1}{\sqrt{d}} \mathbf{H} \mathbf{W}_q \mathbf{W}_k^T \mathbf{X}^T\right) \mathbf{Y} \mathbf{W}_v = \text{softmax}(\mathbf{W}_1 \mathbf{X}^T) \mathbf{Y} \mathbf{W}_v, \quad (4)$$

where we merge the learnable matrices of query  $\mathbf{H}$ , query weight  $\mathbf{W}_q$  and key weight  $\mathbf{W}_k$  as a single matrix  $\mathbf{W}_1$ .

Correspondingly, the cross-attention in the decoder has a learnable key matrix that represents sample positions in the latent space. Therefore, the decoder in (3) is written as

$$\mathbf{U} = \text{softmax}\left(\frac{1}{\sqrt{d}} \mathbf{P} \mathbf{W}_q' \mathbf{W}_k'^T \mathbf{H}^T\right) \mathbf{Z}^L \mathbf{W}_v' = \text{softmax}(\mathbf{P} \mathbf{W}_2^T) \mathbf{Z}^L \mathbf{W}_v'. \quad (5)$$

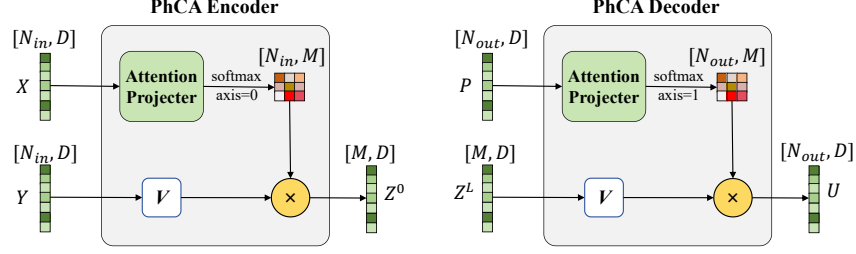


Figure 2: The working mechanism of Physics-Cross-Attention in encoder and decoder respectively.

In addition, utilizing the relationship of the encoder and decoder as mutually inverse transformations, we set  $\mathbf{W}_1 = \mathbf{W}_2$  to reduce the number of parameters, which also improves model performance experimentally. Practically, we generalize the linear projection  $\mathbf{W}_1, \mathbf{W}_2$  with an MLP for further improvement, which is named attention-projector as shown in Figure 2.

In the special case where the input only contains sample positions without physics quantities, our PhCA module is similar to the transformation of physics-aware token in Transolver [23] (only differing in normalizations). In general cases when the inputs include both positions and physics quantities, the two approaches are different. Specifically, in Transolver, the key  $\mathbf{X}$  in (4) and query  $\mathbf{P}$  in (5) contain both positions and physics quantities information, whereas in PhCA, the key matrix  $\mathbf{X}$  in the encoder and the query matrix  $\mathbf{P}$  in the decoder only depend on the positions of the input and output respectively. The physics quantities are used only to produce the value matrix. Such decoupling property of values and locations in query and key enables LNO to predict values at different positions from input positions.

## 4 Experiments

We first evaluate the accuracy for the forward problems on the six popular public benchmarks and for the inverse problem using Burger’s equation. Then, we measure the efficiency in term of the number of model parameters, GPU memory usage and the training time. Finally, we establish ablation study on the choices of different types of attention mechanisms and sample sizes in latent space. Additional experiments on scaling, sampling rate, and sharing weights between encoder and decoder are included in the appendix.

### 4.1 Accuracy for the forward problems

We conduct experiments for the forward problem on six benchmarks including Darcy and NS2d on regular grids (refer to section 5.2, 5.3 in [14] for details), and Airfoil, Elasticity, Plasticity and Pipe problems on irregular grids (refer to section 4.1–4.5 in [41] for details).

Table 1 shows a comprehensive comparison with previous works who reported their performance on the same benchmarks. Our LNO achieves best accuracy on four benchmarks: Darcy, NS2d, Elasticity and Pipe. On the Airfoil and Plasticity benchmarks, our LNO achieves performance close to the SOTA with only half computational cost discussed in Section 4.3. These results demonstrate the effectiveness of approximating the kernel integral operator in the latent space through PhCA module.

### 4.2 Accuracy for the inverse problem

To demonstrate the flexibility of LNO, we design an inverse problem. Given a set of partially observed solution  $u(x)$ , the aim is to recovery the complete  $u(x)$  in a larger domain. Specifically, we test on 1D Burgers’ equation

$$\begin{aligned} \frac{\partial}{\partial t} u(x, t) &= 0.01 \frac{\partial^2}{\partial x^2} u(x, t) - u(x, t) \frac{\partial}{\partial x} u(x, t), \quad x \in [0, 1], \quad t \in [0, 1] \\ u(x, 0) &\sim \text{GaussianProcess}(0, \exp(-\frac{2}{p^{1/2}} \sin^2(\pi||x - x'|)|)), \quad u(0, t) = u(1, t) \end{aligned}$$

The ground-truth data is generated on a  $128 \times 128$  grid with the periodic boundary condition. Initial conditions are sampled from the Gaussian process with the periodic length  $p = 1$ , scaling factor  $l = 1$ .

Table 1: Prediction error on the six forward problems. The best result is in bold. We reproduce the Transolver by implementing codes independently (marked with \*) besides the results claimed in the original paper[23]. The column labeled D.C. indicates whether the observation positions and prediction positions are decoupled. Standard deviations are computed based on 5 independent trials.

Model	D.C.	Relative L2( $\times 10^{-2}$ )					
		Darcy	NS2d	Airfoil	Elasticity	Plasticity	Pipe
FNO[14]	N	1.08	15.56	/	/	/	/
Geo-FNO[41]	N	1.08	15.56	1.38	2.29	0.74	0.67
U-FNO[42]	N	1.83	22.31	2.69	2.39	0.39	0.56
F-FNO[43]	N	0.77	23.22	0.78	2.63	0.47	0.70
LSM[22]	N	0.65	15.35	0.59	2.18	0.25	0.50
Galerkin[20]	N	0.84	14.01	1.18	2.40	1.20	0.98
OFormer[27]	Y	1.24	17.05	1.83	1.83	0.17	1.68
GNOT[21]	Y	1.05	13.80	0.76	0.86	3.36	0.47
FactFormer[28]	N	1.09	12.14	0.71	/	3.12	0.60
ONO[29]	Y	0.76	11.95	0.61	1.18	0.48	0.52
Transolver[23]	N	0.57	9.00	0.49	0.64	<b>0.12</b>	0.33
Transolver*	N	0.58	8.79	<b>0.47</b>	0.62	0.27	0.31
LNO(Ours)	Y	<b>0.49</b> ( $\pm 0.01$ )	<b>8.45</b> ( $\pm 0.22$ )	0.51 ( $\pm 0.05$ )	<b>0.52</b> ( $\pm 0.03$ )	0.29 ( $\pm 0.03$ )	<b>0.26</b> ( $\pm 0.03$ )

The objective of this inverse problem is to reconstruct the complete solution  $u(x)$  in the whole spatiotemporal domain  $(x, t) \in [0, 1] \times [0, 1]$  based on sparsely random-sampled or fixed observation in the sub-spatiotemporal domain  $(x, t) \in [0, 1] \times [0.25, 0.75]$ , as illustrated in Figure 6 in the appendix.

Instead of naive approach which directly learns the mapping from partially observed samples in the subdomain to the complete solution in the whole domain, we propose a two-stage strategy. First, we train the model as a completer to interpolate the solution in the subdomain. Then, we train the model as a propagator to extrapolate from the subdomain to the whole domain. Since, the observation and the prediction samples locate in different positions, only the models with decoupling property can be used as the completer and propagator.

We compare the performance of our LNO with DeepONet[13] and GNOT[21] in two stages respectively. The results in Table 2 and Table 3 indicate that i) in the first stage, LNO performs significantly better than DeepONet and GNOT at different random observation ratio; ii) in the second stage, LNO performs better when the complete solution in the subdomain approaches the ground truth, and the performance degrades as the reconstruction error of the complete solution in the subdomain increases. This is reasonable since we train the propagator based on the ground truth in the sub domain. When there is a significant discrepancy between the ground truth and the prediction of completer, the model faces challenging distribution shifts. Nevertheless, when LNO is used both as the completer and propagator, it achieves the most accurate results for solving this inverse problem.

We also investigate the impact of different temporal and spatial sampling intervals on the accuracy of LNO in the fixed grid observation situation. See appendix B for details.

Table 2: Relative MAE of different completers in the subdomain in the 1st stage of the inverse problem with different settings of observation ratio.

Completer   Observation ratio	20%	10%	5%	1%	0.5%
DeepONet[13]	2.51%	2.59%	2.82%	3.25%	4.82%
GNOT[21]	1.12%	1.39%	1.62%	1.63%	2.56%
LNO(Ours)	<b>0.60%</b>	<b>0.74%</b>	<b>0.77%</b>	<b>1.18%</b>	<b>2.05%</b>

Table 3: The reconstruction error of different propagators in the 2nd stage of the inverse problem. Propagators trained to reconstruct the solution in the whole domain based on the ground truth (G.T.) of the subdomain and are tested using the output of different completers. Relative MAE of  $t = 0$  and  $t = 1$  is reported.

Propagator   Completer	G.T.	LNO		GNOT		DeepONet	
		10%	1%	10%	1%	10%	1%
DeepONet[13]	7.34%	8.01%	9.38%	9.09%	10.80%	11.14%	13.87%
GNOT[21]	5.45%	6.50%	8.07%	<b>8.04%</b>	<b>9.91%</b>	<b>10.41%</b>	<b>13.45%</b>
LNO(Ours)	<b>3.73%</b>	<b>5.69%</b>	<b>7.72%</b>	9.03%	10.98%	13.11%	15.50%

Table 4: Comparison of efficiency between LNO and Transolver on the six forward problem benchmarks. Three metrics are measured: number of parameters, cost of GPU memory and cost of training time per epoch.

Metric	Model	Darcy	NS2d	Airfoil	Elasticity	Plasticity	Pipe
Paras Count(M)	Transolver	1.91	5.33	1.91	1.91	1.91	1.91
	LNO	<b>0.76</b>	<b>5.08</b>	<b>1.36</b>	<b>1.42</b>	<b>1.36</b>	<b>1.36</b>
Memory(GB)	Transolver	17.11	17.17	4.49	1.48	18.41	5.94
	LNO	<b>5.75</b>	<b>7.58</b>	<b>2.47</b>	<b>1.39</b>	<b>7.16</b>	<b>2.89</b>
Time(s/epoch)	Transolver	88.68	107.62	19.49	5.66	83.43	25.56
	LNO	<b>38.98</b>	<b>57.83</b>	<b>9.35</b>	<b>5.33</b>	<b>41.62</b>	<b>14.13</b>

### 4.3 Efficiency

We demonstrate improvement on efficiency of our proposed LNO compared to Transolver, which was considered the most efficient Transformer-based PDE solvers[23]. Results in Table 4 indicate that our method has fewer parameters, lower memory consumption, and faster training speed. Roughly speaking, LNO reduces the parameter count by an average of 30% and memory consumption by 50% compared to Transolver across all benchmarks, also with a 1.8x training speed up.

The improvement of LNO stems from the idea of solving PDEs in the latent space. Given  $N$  input points in real-world space, if both of Transolver and LNO are consisted of  $L$  Transformer blocks, the Transolver, which applies Physics-Attention in each block, has the time complexity of  $O(LMN + LM^2)$ , where  $M$  is the number of slices. Our LNO, which applies Physics-Cross-Attention only in the encoder and decoder, has the time complexity of  $O(MN + LM^2)$ , where  $M$  is the sample size in latent space.

### 4.4 Ablation Study

**Necessity of decoupling** Decoupling the values and locations as well as the observation positions and prediction positions not only guarantees the flexibility but also improves the accuracy. To study the effect of decoupling property, we replaces the PhCA in LNO by Physics-Attention proposed in Transolver[23]. In this way, the query and keys are calculated from the same embedding of both  $pos_{in}$  and  $val_{in}$  of input sequence. The  $pos_{out}$  which not presents in the input sequence can not generate queries and keys. So the observation positions and prediction positions must be kept the same. We compare the performance of LNO with PhCA or Physics-Attention on the forward problem benchmarks, and the results in the first and last rows of Table 5 verify the necessity of decoupling.

**Expressiveness of quadratic attention** We study the impact on accuracy using different attention mechanisms in the latent space. We replace the scaled dot-product attention in LNO with Galerkin-type attention used in Galerkin Transformer[20], efficient attention[18] used in GNOT[21], and Nystrom attention[19] used in ONO[29]. The comparison results in Table 5 show that quadratic attention such as scaled dot-product attention[16] is more expressive than linear attention, which helps improve the accuracy. Many previous methods have employed different linear attentions[20, 21, 29] to reduce the computational costs at the expense to reduce the accuracy. Since the length of the latent



sample sequence is much smaller than the inputs and outputs in real-world space, therefore, applying quadratic attention in latent space does not incur significant overhead.

Table 5: The ablation results using different attention implementation. P.A. stands for Physics-Attention. E.A. stands for Efficient Attention, N.A. stands for Nystrom Attention and G.A. stands for Galerkin-type Attention.

Model	Relative L2( $\times 10^{-2}$ )					
	Darcy	NS2d	Airfoil	Elasticity	Plasticity	Pipe
LNO with P.A.[23]	0.53	22.65	0.74	0.88	0.49	0.40
LNO with E.A.[18, 21]	0.63	20.18	0.59	0.54	0.44	0.36
LNO with N.A.[19, 29]	0.67	23.03	0.63	0.79	0.30	0.48
LNO with G.A.[20]	0.71	22.44	0.89	0.93	0.43	0.39
<b>LNO</b>	<b>0.49</b>	<b>8.45</b>	<b>0.51</b>	<b>0.52</b>	<b>0.29</b>	<b>0.26</b>

**Sample size in latent space** We investigate the impact of sample size in latent space on LNO for solving both the forward and inverse problems. Results are shown in Figure 3. In the forward problems, as the sample size  $M$  in latent space increases, the performance of LNO gradually improves to a saturation level, followed by a gentle decline on the benchmarks of Airfoil, Elasticity, Plasticity, and Pipe. However, on benchmarks of Darcy and NS2d, the performance of LNO continues to improve till  $M = 512$ . This may be attributed to the former set of benchmarks containing only location information, while the latter set involves both location and physics quantity information, which requires more samples to represent. In the inverse problem, the performance of completer and propagator are similar to the trends in the forward problems.

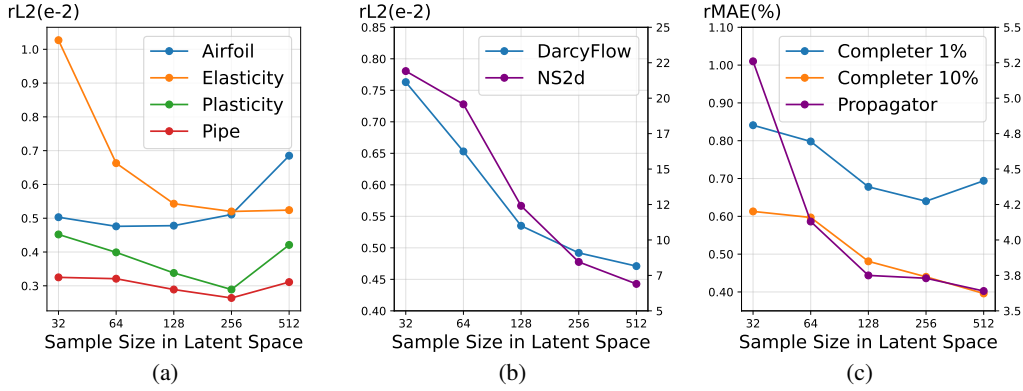


Figure 3: Sample size in latent space v.s. accuracy. (a) Forward problems on Airfoil, Elasticity, Plasticity, Pipe. (b) Forward problems on Darcy, NS2d. (c) Inverse Problem.

## 5 Conclusions

The paper explores the feasibility of characterizing PDEs in a learnable latent space. We present **Physics-Cross-Attention (PhCA)** for encoding inputs into the latent space and for decoding outputs. We build the **Latent Neural Operator (LNO)** based on PhCA and validate its flexibility, efficiency and accuracy for solving both forward and inverse problems. In this work, no prior is imposed on the latent space, but, in future, it is worthy to explore whether physical priors, e.g. symmetry or disentanglement, can help gain further improvements, and explore generalization ability of PhCA crossing domains and re-usability for multiple types of PDEs.

## References

- [1] Jaideep Pathak, Shashank Subramanian, Peter Harrington, Sanjeev Raja, Ashesh Chattopadhyay, Morteza Mardani, Thorsten Kurth, David Hall, Zongyi Li, Kamyar Azizzadenesheli, et al. FourCastNet: a global data-driven high-resolution weather model using adaptive Fourier neural operators. *arXiv preprint arXiv:2202.11214*, 2022.
- [2] Zhenze Yang, Chi-Hua Yu, and Markus J Buehler. Deep learning model to predict complex stress and strain fields in hierarchical composites. *Science Advances*, 7(15):eabd7416, 2021.
- [3] Yifan Mei, Yijie Zhang, Xueyu Zhu, and Rongxi Gou. Forward and inverse problems for eikonal equation based on DeepONet. *arXiv preprint arXiv:2306.05754*, 2023.
- [4] Timothy Praditia, Matthias Karlbauer, Sebastian Otte, Sergey Oladyshkin, Martin V Butz, and Wolfgang Nowak. Learning groundwater contaminant diffusion-sorption processes with a finite volume neural network. *Water Resources Research*, 58(12):e2022WR033149, 2022.
- [5] Junuthula Narasimha Reddy. An introduction to the finite element method. *New York*, 27:14, 1993.
- [6] Zhongkai Hao, Songming Liu, Yichi Zhang, Chengyang Ying, Yao Feng, Hang Su, and Jun Zhu. Physics-informed machine learning: a survey on problems, methods and applications. *arXiv preprint arXiv:2211.08064*, 2022.
- [7] Maziar Raissi, Paris Perdikaris, and George E Karniadakis. Physics-informed neural networks: a deep learning framework for solving forward and inverse problems involving nonlinear partial differential equations. *Journal of Computational Physics*, 378:686–707, 2019.
- [8] Matthias Karlbauer, Timothy Praditia, Sebastian Otte, Sergey Oladyshkin, Wolfgang Nowak, and Martin V Butz. Composing partial differential equations with physics-aware neural networks. In *Proceedings of the International Conference on Machine Learning (ICML)*, 2022.
- [9] Craig R Gin, Daniel E Shea, Steven L Brunton, and J Nathan Kutz. DeepGreen: deep learning of Green’s functions for nonlinear boundary value problems. *Scientific Reports*, 11(1):21614, 2021.
- [10] Chengping Rao, Pu Ren, Qi Wang, Oral Buyukozturk, Hao Sun, and Yang Liu. Encoding physics to learn reaction–diffusion processes. *Nature Machine Intelligence*, 5(7):765–779, 2023.
- [11] Sifan Wang, Hanwen Wang, and Paris Perdikaris. Learning the solution operator of parametric partial differential equations with physics-informed DeepONets. *Science Advances*, 7(40):eabi8605, 2021.
- [12] Tianping Chen and Hong Chen. Universal approximation to nonlinear operators by neural networks with arbitrary activation functions and its application to dynamical systems. *IEEE Transactions on Neural Networks*, 6(4):911–917, 1995.
- [13] Lu Lu, Pengzhan Jin, and George Em Karniadakis. DeepONet: learning nonlinear operators for identifying differential equations based on the universal approximation theorem of operators. *arXiv preprint arXiv:1910.03193*, 2019.
- [14] Zongyi Li, Nikola Kovachki, Kamyar Azizzadenesheli, Burigede Liu, Kaushik Bhattacharya, Andrew Stuart, and Anima Anandkumar. Fourier neural operator for parametric partial differential equations. *arXiv preprint arXiv:2010.08895*, 2020.
- [15] Nikola Kovachki, Zongyi Li, Burigede Liu, Kamyar Azizzadenesheli, Kaushik Bhattacharya, Andrew Stuart, and Anima Anandkumar. Neural operator: learning maps between function spaces with applications to PDEs. *Journal of Machine Learning Research*, 24(89):1–97, 2023.
- [16] Ashish Vaswani, Noam Shazeer, Niki Parmar, Jakob Uszkoreit, Llion Jones, Aidan N Gomez, Łukasz Kaiser, and Illia Polosukhin. Attention is all you need. In *Advances in Neural Information Processing Systems (NeurIPS)*, 2017.
- [17] Georgios Kissas, Jacob H Seidman, Leonardo Ferreira Guilhoto, Victor M Preciado, George J Pappas, and Paris Perdikaris. Learning operators with coupled attention. *Journal of Machine Learning Research*, 23(215):1–63, 2022.
- [18] Zhuoran Shen, Mingyuan Zhang, Haiyu Zhao, Shuai Yi, and Hongsheng Li. Efficient attention: attention with linear complexities. In *Proceedings of the IEEE/CVF Winter Conference on Applications of Computer Vision (WACV)*, 2021.

- [19] Yunyang Xiong, Zhanpeng Zeng, Rudrasish Chakraborty, Mingxing Tan, Glenn Fung, Yin Li, and Vikas Singh. Nyströmformer: a Nyström-based algorithm for approximating self-attention. In *Proceedings of the AAAI Conference on Artificial Intelligence (AAAI)*, 2021.
- [20] Shuhao Cao. Choose a transformer: Fourier or Galerkin. In *Advances in Neural Information Processing Systems (NeurIPS)*, 2021.
- [21] Zhongkai Hao, Zhengyi Wang, Hang Su, Chengyang Ying, Yinpeng Dong, Songming Liu, Ze Cheng, Jian Song, and Jun Zhu. GNOT: a general neural operator Transformer for operator learning. In *Proceedings of the International Conference on Machine Learning (ICML)*, 2023.
- [22] Haixu Wu, Tengge Hu, Huakun Luo, Jianmin Wang, and Mingsheng Long. Solving high-dimensional PDEs with latent spectral models. *arXiv preprint arXiv:2301.12664*, 2023.
- [23] Haixu Wu, Huakun Luo, Haowen Wang, Jianmin Wang, and Mingsheng Long. Transolver: a fast Transformer solver for PDEs on general geometries. *arXiv preprint arXiv:2402.02366*, 2024.
- [24] Benedikt Alkin, Andreas Fürst, Simon Schmid, Lukas Gruber, Markus Holzleitner, and Johannes Brandstetter. Universal physics Transformers. *arXiv preprint arXiv:2402.12365*, 2024.
- [25] Somdatta Goswami, Katiana Kontolati, Michael D Shields, and George Em Karniadakis. Deep transfer operator learning for partial differential equations under conditional shift. *Nature Machine Intelligence*, 4(12):1155–1164, 2022.
- [26] Zongyi Li, Nikola Kovachki, Kamyar Azizzadenesheli, Burigede Liu, Kaushik Bhattacharya, Andrew Stuart, and Anima Anandkumar. Neural operator: graph kernel network for partial differential equations. *arXiv preprint arXiv:2003.03485*, 2020.
- [27] Zijie Li, Kazem Meidani, and Amir Barati Farimani. Transformer for partial differential equations’ operator learning. *arXiv preprint arXiv:2205.13671*, 2022.
- [28] Zijie Li, Dule Shu, and Amir Barati Farimani. Scalable Transformer for PDE surrogate modeling. In *Advances in Neural Information Processing Systems (NeurIPS)*, 2024.
- [29] Zipeng Xiao, Zhongkai Hao, Bokai Lin, Zhijie Deng, and Hang Su. Improved operator learning by orthogonal attention. *arXiv preprint arXiv:2310.12487*, 2023.
- [30] Franco Scarselli, Marco Gori, Ah Chung Tsoi, Markus Hagenbuchner, and Gabriele Monfardini. The graph neural network model. *IEEE Transactions on Neural Networks*, 20(1):61–80, 2008.
- [31] Ruchi Guo, Shuhao Cao, and Long Chen. Transformer meets boundary value inverse problems. In *Proceedings of the International Conference on Learning Representations (ICLR)*, 2022.
- [32] Guanchao Liu, Lei Zhang, Qingzhen Wang, and Jianhua Xu. Data-driven seismic prestack velocity inversion via combining residual network with convolutional autoencoder. *Journal of Applied Geophysics*, 207:104846, 2022.
- [33] Bin Liu, Yuxiao Ren, Hanchi Liu, Hui Xu, Zhengfang Wang, Anthony G Cohn, and Peng Jiang. GPRInvNet: deep learning-based ground-penetrating radar data inversion for tunnel linings. *IEEE Transactions on Geoscience and Remote Sensing*, 59(10):8305–8325, 2021.
- [34] Zhongping Zhang, Yue Wu, Zheng Zhou, and Youzuo Lin. VelocityGAN: subsurface velocity image estimation using conditional adversarial networks. In *Proceedings of the IEEE Winter Conference on Applications of Computer Vision (WACV)*, 2019.
- [35] Juri Ranieri, Amina Chebira, Yue M Lu, and Martin Vetterli. Sampling and reconstructing diffusion fields with localized sources. In *Proceedings of the IEEE International Conference on Acoustics, Speech and Signal Processing (ICASSP)*, 2011.
- [36] Hassan Bararnia and Mehdi Esmaeilpour. On the application of physics informed neural networks (PINN) to solve boundary layer thermal-fluid problems. *International Communications in Heat and Mass Transfer*, 132(8):105890, 2022.
- [37] Shengze Cai, Zhicheng Wang, Chrysostomos Chrysostomidis, and George Em Karniadakis. Heat transfer prediction with unknown thermal boundary conditions using physics-informed neural networks. In *Proceedings of the Fluids Engineering Division Summer Meeting (FEDSM)*, 2020.
- [38] Hongping Wang, Yi Liu, and Shizhao Wang. Dense velocity reconstruction from particle image velocimetry/particle tracking velocimetry using a physics-informed neural network. *Physics of Fluids*, 34(1):017116, 2022.

- [39] Roberto Molinaro, Yunan Yang, Björn Engquist, and Siddhartha Mishra. Neural inverse operators for solving PDE inverse problems. *arXiv preprint arXiv:2301.11167*, 2023.
- [40] Coşku Can Horuz, Matthias Karlbauer, Timothy Praditia, Martin V Butz, Sergey Oladyshkin, Wolfgang Nowak, and Sebastian Otte. Inferring boundary conditions in finite volume neural networks. In *Proceedings of the International Conference on Artificial Neural Networks (ICANN)*, 2022.
- [41] Zongyi Li, Daniel Zhengyu Huang, Burigede Liu, and Anima Anandkumar. Fourier neural operator with learned deformations for PDEs on general geometries. *Journal of Machine Learning Research*, 24(388):1–26, 2023.
- [42] Gege Wen, Zongyi Li, Kamyar Azizzadenesheli, Anima Anandkumar, and Sally M Benson. U-FNO—an enhanced Fourier neural operator-based deep-learning model for multiphase flow. *Advances in Water Resources*, 163:104180, 2022.
- [43] Alasdair Tran, Alexander Mathews, Lexing Xie, and Cheng Soon Ong. Factorized Fourier neural operators. *arXiv preprint arXiv:2111.13802*, 2021.
- [44] Ilya Loshchilov and Frank Hutter. Decoupled weight decay regularization. In *Proceedings of the International Conference on Learning Representations (ICLR)*, 2018.
- [45] Leslie N Smith and Nicholay Topin. Super-convergence: very fast training of neural networks using large learning rates. In *Artificial Intelligence and Machine Learning for Multi-Domain Operations Applications*, 2019.

## A Scaling Experiments

We conduct scaling experiments to investigate the impact of model depth (number of stacked Transformer blocks) and model width (dimension of tokens in Transformer blocks) on the performance of LNO.

As shown in Figure 4, with model depth increasing, the performance of LNO initially improves and then declines, reaching its optimal performance at 4 or 8. This suggests that deeper LNO encounters optimization challenges in solving PDEs in the latent space. Simply stacking more Transformer blocks does not necessarily lead to better accuracy.

As shown in Figure 5, although the performance of LNO continues benefiting from increasing model width, it gradually exhibits a saturation trend when the dimension of tokens reaches as large as 256.

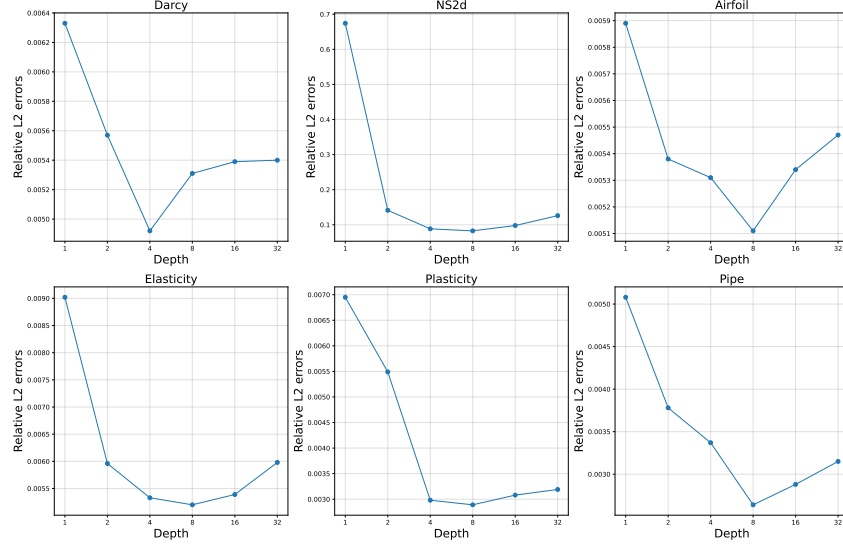


Figure 4: The influence of model depth on the performance of LNO across six forward problem benchmarks.

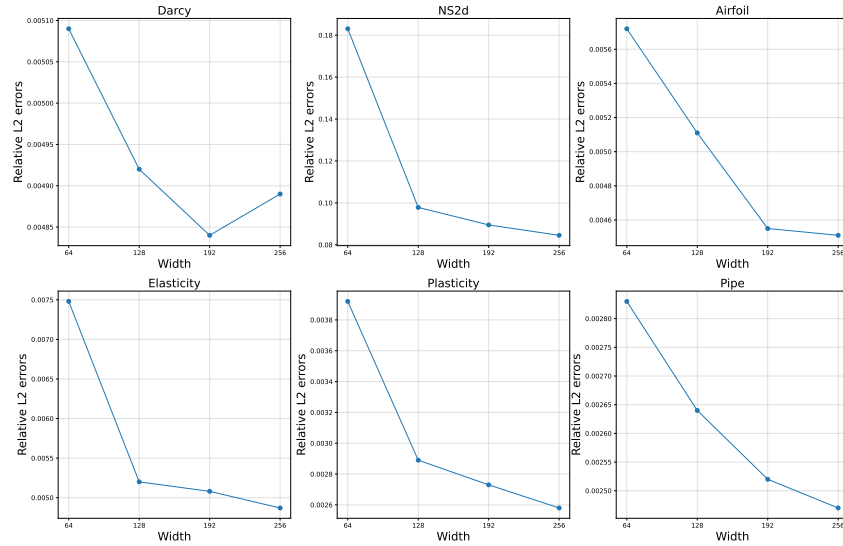


Figure 5: The influence of model width on the performance of LNO across six forward problem benchmarks.

## B Observation Ratio and Locations for the Inverse PDE Task

We investigate the impact of different temporal and spatial sampling intervals on the accuracy of LNO when solving inverse problem in the fixed observation situation. As shown by Figure 8, it can be found that i) the inverse problem can still be solved accurately even when the temporal and spatial sampling intervals are both as large as 16 (approximately only 0.4% observation ratio); ii) the increase of the spatial sampling interval significantly compromises the solution accuracy compared to that of the temporal sampling interval; iii) spatial undersampling can hardly be compensated for through temporal oversampling.

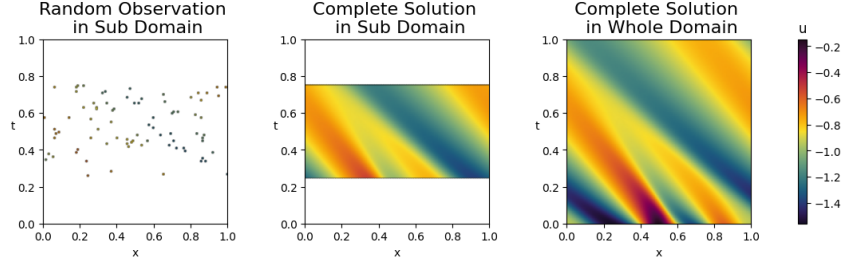


Figure 6: Visualization of Burgers' equation with different observation situations in different regions. We propose a two-stage strategy. First, we interpolate the solution in the subdomain. Then, we extrapolate from the subdomain to the whole domain.

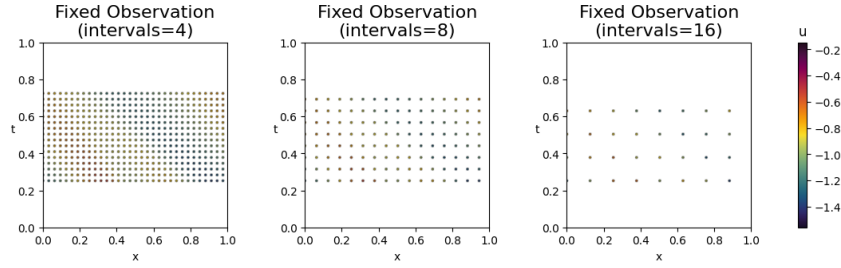


Figure 7: Visualization of Burgers' equation in the fixed observation situation with different temporal and spatial sampling intervals.

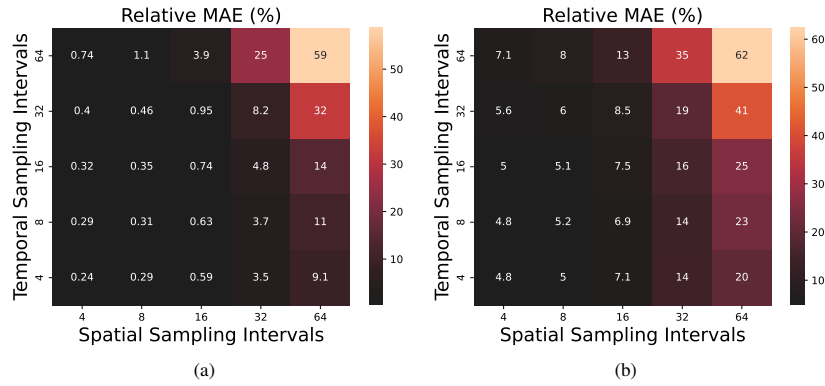


Figure 8: Accuracy of solving inverse problem at different temporal and spatial sampling intervals. (a) Accuracy of LNO as completer. (b) Accuracy of LNO as propagator based on the results of corresponding completer.

## C Additional Ablation Study

We conduct additional ablation study to explore the performance of LNO when  $W_1 \neq W_2$  in (4) and (5). In this way, we replace the linear projection  $W_1$  and  $W_2$  with two individual MLPs. Results of comparison between LNO using shared MLPs and LNO using non-shared MLPs in PhCA encoder and decoder are shown in Table 6. It can be found that LNO performs better on most benchmarks (except Plasticity) under the shared situation.

Table 6: The ablation results on six forward problem benchmarks. Relative L2 is recorded. Smaller values represent better performance. The better result is in bold.

Model	Relative L2( $\times 10^{-2}$ )					
	Darcy	NS2d	Airfoil	Elasticity	Plasticity	Pipe
LNO(non-shared)	0.54	10.67	0.53	1.09	<b>0.26</b>	0.36
LNO	<b>0.49</b>	<b>8.45</b>	<b>0.51</b>	<b>0.52</b>	0.29	<b>0.26</b>

## D Full Implementation Details

The full implementation details of LNO in both forward and inverse problems are shown in Table 7. All the experiments are conducted on single or two NVIDIA RTX 3090 GPUs.

For the forward problems, we train the models using relative L2 error for 500 epochs. AdamW optimizer[44] and OneCycleLr scheduler[45] are applied with initial learning rate at  $10^{-3}$ . We reproduced the results of Transolver[23] following implementations in appendix B.3 in [23] and also excerpt the results of other methods from Table 2 in [23]. The data splits are the same as in appendix B.1 in [23].

For the inverse problem, we train the models using mean squared error and StepLr scheduler as well. For DeepONet[13], we use 4 Transformer blocks with 128-dimensional tokens as the branch net and 3 fully-connected layers as the trunk net. For GNOT[21], we set the number of Transformer blocks as 4, dimension of tokens as 96, and number of experts as 1. We use 4096 samples for training, 128 samples for validating and 128 samples for testing.

Table 7: The hyperparameters and training configuration of LNO in solving the forward and inverse problems in Section 4.1 and 4.2

Benchmark	Layers	Dim	Size	Heads	Batch	Epoch	Loss	Optimizer	Scheduler
Darcy	4	128	256	8	4	500	rL2	AdamW[44]	OneCycleLR[45]
NS2d	8	256							
Airfoil	8	128							
Elasticity	8	128							
Plasticity	8	128							
Pipe	8	128							
Completer Propagator	4	96	256	8	4	500	MSE	AdamW	StepLR